

# Application of Auger Spectroscopy for Measurement of Secondary Electron Emission from Conducting Material for Electric Propulsion Devices

IEPC-2013-320

*Presented at the 33rd International Electric Propulsion Conference,  
The George Washington University • Washington, D.C. • USA  
October 6 – 10, 2013*

Marlene I. Patino<sup>1</sup>  
*University of California, Los Angeles, CA, 90095, USA*

Yevgeny Raitses<sup>2</sup>  
*Princeton Plasma Physics Laboratory, Princeton, NJ, 08543, USA*

Bruce E. Koel<sup>3</sup>  
*Princeton University, Princeton, NJ, 08540, USA*

*and*

Richard E. Wirz<sup>4</sup>  
*University of California, Los Angeles, CA 90095, USA*

**Abstract:** A facility utilizing Auger electron spectroscopy was developed to measure secondary electron emission from conducting materials. Both the total secondary electron emission yield and the energy distribution of the emitted electrons were measured for graphite for primary electron beam energies of 50 to 500eV. The total yield calculated using two different techniques – with the secondary electron emission calculated from current measurements of the sample and from a hemispherical collector - were found to agree well with each other and with a semi-empirical equation for the energies at which the measurements were taken.

## Nomenclature

$\delta$	=	yield of true secondary electrons
$\eta$	=	yield of elastically and inelastically reflected electrons
$\sigma$	=	total secondary electron yield
$\sigma_{cr}$	=	critical total secondary electron yield at which emission is space-charge limited
$\sigma_{max}$	=	maximum total secondary electron yield
$E_{PE}$	=	primary electron beam energy
$E_{PE}^{max}$	=	primary electron beam energy at which the total secondary electron yield is a maximum
$I_{PE}$	=	primary electron beam current
$I_{RE}$	=	current of elastically and inelastically reflected electrons

---

<sup>1</sup> Graduate Student, Department of Mechanical and Aerospace Engineering, mipatino@ucla.edu.

<sup>2</sup> Principal Research Physicist, Princeton Plasma Physics Laboratory, yraitses@pppl.gov.

<sup>3</sup> Professor, Department of Chemical and Biological Engineering, bkoel@princeton.edu.

<sup>4</sup> Assistant Professor, Department of Mechanical and Aerospace Engineering, wirz@ucla.edu.

Copyright © 2013 by Marlene Patino. Published by the Electric Rocket Propulsion Society with permission.

$I_{SE}$  = current of true secondary electrons  
 $I_{collector}$  = collector current  
 $I_{sample}$  = sample current

## I. Introduction

**E**LECTRON bombardment of materials can lead to the emission of electrons from the materials (termed secondary electron emission) by various processes (Fig. 1) and can be separated by their energies (Fig. 2). Backscattered electrons are reflected after experiencing elastic collisions with valence electrons of the surface material, and are at approximately the primary electron energy. Inelastically reflected electrons with energies between 50eV and the primary electron energy are created during Auger transitions and plasmon generation.<sup>1</sup> True secondaries with energies below 50eV are produced by the ionization of atoms within the material by primary and reflected electrons.

Secondary electron emission (SEE) from electron bombardment of materials can have adverse effects at a plasma-material interface (e.g. in electric propulsion, fusion, and plasma-processing devices), where SEE from the wall decreases the potential at the wall and hence increases electron loss to the wall, heating of the wall, and cooling of the plasma.<sup>2-4</sup> The emitted electrons can also form beams due to their acceleration in the sheath, which for particular energy distributions of emitted electrons and beam and plasma electron densities, can lead to a two-stream instability.<sup>5</sup> In particle accelerators, the SEE may lead to instabilities in the positron beam and, depending on the emission behavior at low primary electron energies, may also lead to overheating of critical facility components (e.g. superconducting magnets).<sup>6</sup> The behavior of the total yield at low primary energies is a subject of much controversy<sup>7</sup> and will not be discussed in the present paper.

Over the past century, extensive studies on SEE from materials have been performed. Many relations, mostly empirical, were developed for the dependence of total secondary electron yield (i.e. the number of secondary electrons emitted per incident primary electron) on the energy<sup>6,8-14</sup> and angle<sup>1,9</sup> of the primary electrons with respect to the material surface, and for the energy,<sup>15</sup> angle, and spatial distribution of the secondary electrons.

Zamoski et al<sup>16</sup> calculated the dependence of total yield on primary electron energy for pocographite by monitoring the current on the target. Pedgley and McCracken<sup>13</sup> and Belhaj et al<sup>17</sup> calculated total yields of 5890 PT graphite and graphite, respectively, by monitoring the current on a cylindrical and hemispherical collector; Pedgley and McCracken were also able to calculate true secondary yield by separating the contributions of true and reflected secondary electrons. A 4-grid plus collector hemispherical assembly designed for surface analysis was used as a collector by Woods et al,<sup>18,19</sup> Farhang et al,<sup>14</sup> and Kirby<sup>20</sup> to calculate true secondary yield of AXP-5Q pocographite, 5890 PT graphite, and AXF-5W pocographite, respectively; section IIA provides more detail on such a grid-collector assembly.

The disadvantages of SEE discussed above have led to the investigation of various forms of carbon for electric propulsion devices due to its low SEE properties and low sputtering. Graphite and carbon-carbon composite were examined for grids in ion thrusters.<sup>21,22</sup> Hall thrusters with segmented carbon velvet<sup>23</sup> and layered graphite/boron nitride<sup>24</sup> channels were built and tested. As higher power electric propulsion devices become more abundant, the use of graphite becomes more important since the primary electron energy at which the sheath will disappear for a xenon plasma (due to the increase in wall potential mentioned previously)<sup>2</sup> is larger for graphite than for most other materials.

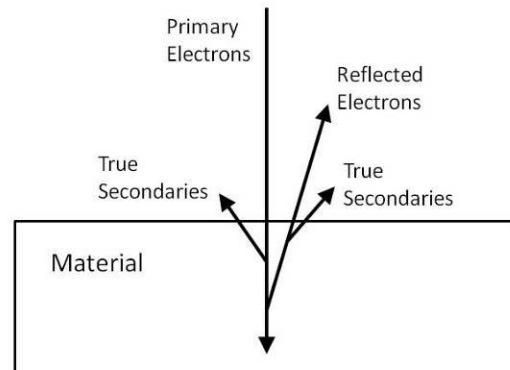


**Figure 1. Emission of secondary electrons (reflected and true secondaries) due to bombardment with primary electrons.**

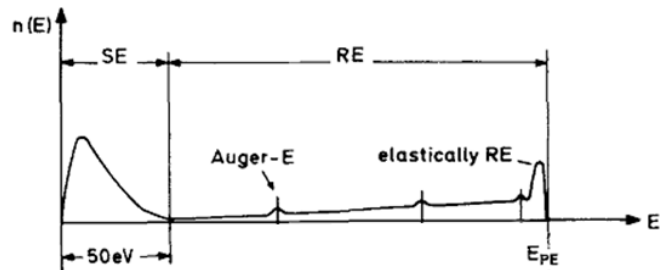


**Figure 2. Secondary electron energy distribution (adapted from Ref. 1).**

This paper summarizes the research effort conducted at the Princeton Plasma Physics Laboratory (PPPL) to determine the feasibility of using surface analysis instruments as used by Refs. 18-20 for measuring the SEE properties of conducting materials. Detailed measurements of the SEE produced from graphite due to electron bombardment at primary electron energies between 50 and 500eV are presented.

Section II of this paper introduces the experimental setup and approach whereby the SEE measurements are taken. Section IIIA provides results of the characterization (i.e. size, shape, and current) of the primary electron beam. In Section IIIB, the total secondary yield of graphite is calculated and compared with existing experimental data. The secondary electron energy distribution is then used to separate contributions from low-energy true secondary electrons and higher energy reflected electrons. The paper concludes in Section IV with a discussion of proposed primary electron beam energies and materials for future SEE measurements.

## II. Experimental Setup

This section reviews the high vacuum facility with base pressure  $5 \times 10^{-8}$  Torr, developed for measuring SEE, including the grid-collector assembly. Brief description of the phosphor screen used for beam characterization and details on the sample mounting system are also provided.

### A. LEED-AES system

The experiment utilized a four-grid plus collector assembly (Fig. 3) commonly used to study the structure and composition of material surfaces by low-energy electron diffraction (LEED) and Auger electron spectroscopy (AES), respectively. These surface analysis instruments provide excellent shielding of electrons from environmental effects (e.g. the Earth's magnetic field) and hence are ideal for such high sensitivity experiments as SEE.

The LEED-AES Phi model 15-120 system provides primary electrons with energies of up to 1600eV through a thermionic emission electron gun. The secondary electrons produced were measured on the collector with a Keithley 6485 picoammeter; note that only  $120^\circ$  collection angle measurements are obtained with the LEED-AES system used. A negative potential was applied at grids G2 and G3 with an Ortec 556 high voltage power supply to prevent secondary electrons with energy below the applied potential from reaching the collector. Hence the system works as a high pass filter and a distribution of the energy of the secondary electrons was obtained as the applied potential was varied. Grid G1 was kept at ground potential to maintain a field free region between the sample and collector.

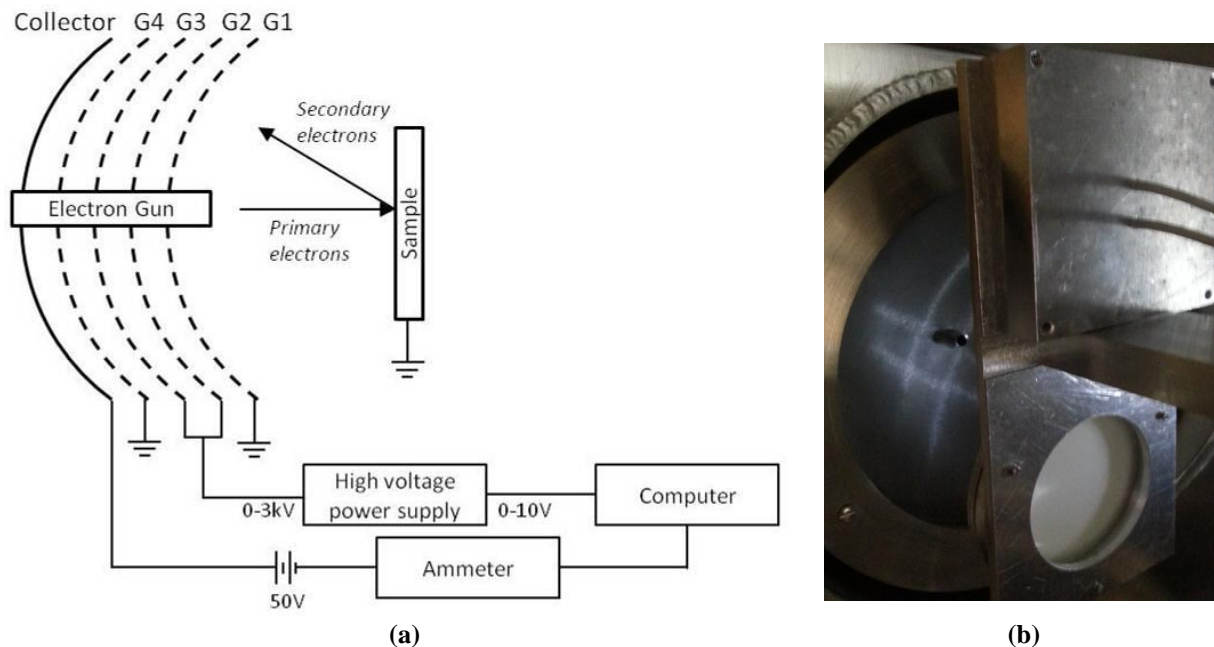


Figure 3. (a) Schematic and (b) picture of the facility for measuring SEE, including AES electron optics.



**Figure 4. (a) Sample and (b) phosphor screen.**

### **B. Mounting system**

The sample and a phosphor screen were mounted on a grounded plate (Fig. 4) approximately 20mm downstream of the LEED-AES system. The plate was attached to a vertical stage to move the sample or the phosphor screen in front of the electron gun and was designed such that the surface of the sample and phosphor screen were equidistant from the electron gun.

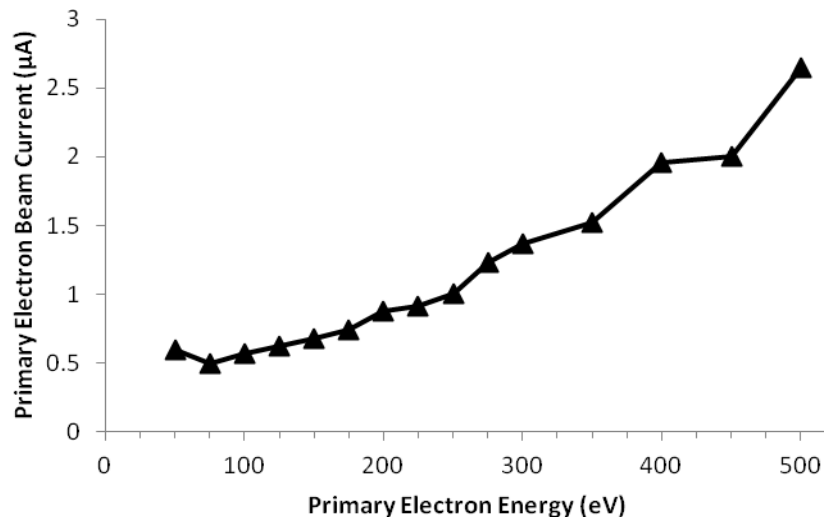
The sample was electrically insulated from the mount to allow biasing of the sample, and precise measurements of sample current independent of any current that may be collected on the mounting plate. A zinc sulfide phosphor screen allowed for visualization of the beam size and shape from a viewport opposite the LEED-AES system; the phosphor screen was grounded via the mounting plate.

## **III. Results and Analysis**

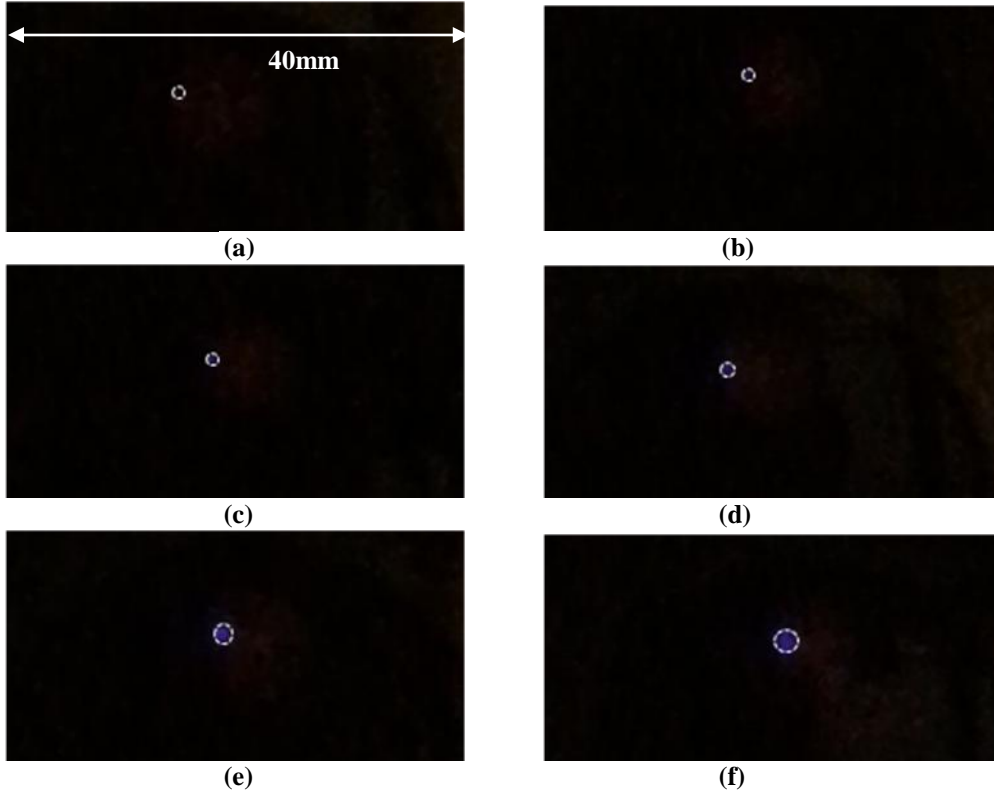
### **A. Electron Beam Characterization**

Figure 5 shows the variation of the electron beam current with primary electron energy from 50 to 500eV. The beam current was determined by measuring the sample current as a positive voltage was increasingly applied to the sample to keep secondary electrons on the sample. The sample current curve was extrapolated down to zero sample voltage to account for any effects the biased sample might have on the primary electrons (e.g. acceleration of the primary electrons leading to changes in yield and energy of reflected electrons). Future measurements of electron beam current will be made with a two concentric cylinder Faraday cup design.

Images of the electron beam on the phosphor screen are found in Figure 6 for primary electron energy of 300 to 600eV. For all present measurements the electron gun was focused at 300eV (below 300eV the electron beam was not visible on the phosphor screen). As can be seen in Figure 6, the electron beam is only slightly defocused from approximately 1mm in diameter at 300eV to 1.7mm at 500eV. In future experiments, the beam will be better focused at each beam energy for greater accuracy.



**Figure 5. Electron beam current as a function of primary electron energy.**



**Figure 6. Image of the electron beam (outlined in white) on the phosphor screen at (a) 300eV, (b) 350eV, (c) 400eV, (d) 450eV, (e) 500eV, and (f) 600eV. Note that the electron beam is less focused at higher energies.**

### B.Secondary Electron Yield

The total secondary electron yield  $\sigma$  was calculated using two different approaches. In the first approach, the measured sample current was used in the calculation

$$\sigma = \frac{I_{SE} + I_{RE}}{I_{PE}} = \frac{I_{PE} - (I_{PE} - I_{SE} - I_{RE})}{I_{PE}} = \frac{I_{PE} - I_{sample}}{I_{PE}} \quad (1)$$

where  $I_{PE}$ ,  $I_{RE}$ , and  $I_{SE}$  are the primary, reflected, and true secondary electron currents and  $I_{sample}$  is the current on the sample when the sample is at ground potential.

In the second approach, the secondary electron current measured on the LEED-AES collector assembly was used to calculate  $\sigma$ ,

$$\sigma = \frac{I_{SE} + I_{RE}}{I_{PE}} = \frac{I_{collector}}{I_{PE}} \quad (2)$$

where  $I_{collector}$  includes the currents on the four grids and the final collector.  $I_{collector}$  was determined by measuring the current on the collector assembly as the first grid G1 was biased positively to ensure complete collection of all secondary electrons. Once again, the collector assembly current curve was extrapolated down to zero voltage on G1 to account for any effects the biased grid may have on the primary electrons (e.g. attracting the primary electrons before reaching the sample).

The total secondary electron yields using both techniques are plotted in Figure 7. Also plotted is a semi-empirical equation for the energy dependence of total secondary electron yield,<sup>11</sup>

$$\sigma(E_{PE}) = \sigma_{max} \exp \left\{ - \left[ \ln \left( \frac{E_{PE}}{E_{PE}^{max}} \right) \right]^2 / 2\alpha^2 \right\} \quad (3)$$

where  $\alpha = 1.6$  and the values for maximum yield,  $\sigma_{max}$ , and primary electron energy at which the yield is a maximum,  $E_{PE}^{max}$ , are taken from the yield calculated from Eqn. 1. From Figure 7, the total yields calculated using

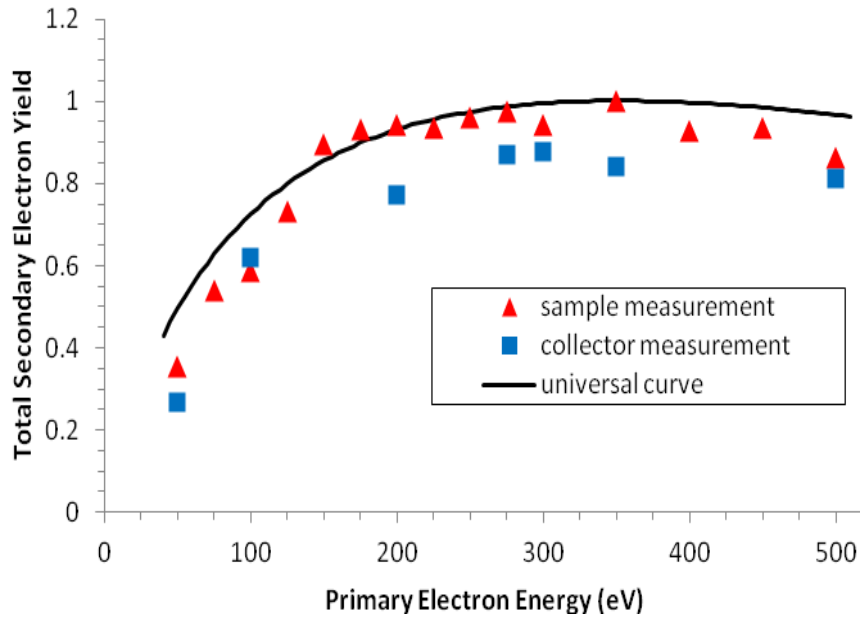


**Figure 7. Secondary electron yield as a function of primary electron energy for graphite calculated using the sample current (triangles) and the collector assembly current (squares) for secondary electron current. The solid line is the semi-empirical universal curve for the total yield from Ref. 11 for the measured  $\sigma_{\max}$  and  $E_{\max}$ .**

Eqns. 1 and 2 compare well with each other and with the semi-empirical equation. Additionally, the secondary electron emission from graphite in a xenon plasma can increase the wall potential such that the sheath disappears for primary electron energies as low as 275eV (where  $\sigma = \sigma_{\text{cr}} = 0.98$ ).

### C. Secondary Electron Energy Spectrum

As mentioned in section IIA, the energy distribution of emitted electrons is obtained by applying a retarding voltage to grids G2 and G3 in front of the collector and measuring the current on the collector. The energy distributions for a 100, 200, 350, and 500eV primary electron beam are found in Figure 8. The large peak at energies below 50eV are attributed to the true secondary electrons created in ionization processes within the material; the smaller peak near the primary electron beam energy are elastically reflected electrons that have lost little to no energy in collisions with the surface atoms. From Figure 8, as the primary electron beam energy is reduced, the percentage of elastically reflected electrons increases.

Note that the integration of the non-normalized energy distribution curve at each primary electron energy does not reproduce the total secondary electron current at that energy. The energy distributions curves are taken from electrons reaching the collector which is located behind 4-grids, representing an effective transparency of 35-45%.

## IV. Conclusion

The use of Auger electron spectroscopy instruments for fully characterizing the secondary electron emission (yield and energy distribution of emitted electrons) of conducting materials was validated with measurements of graphite for primary electron beam energies between 50 and 500eV. Accurate measurements required that the LEED-AES system grid transparency be considered, as well as the effects of sample biasing on the electron gun.

Future experiments will investigate the behavior of reflected electrons at low primary electron energies. In particular, experiments will determine if the yield goes to zero as the primary electron energy goes to zero as is assumed in many semi-empirical equations of total secondary electron yield, or if the instead the total yield has a minimum below 20eV and goes to 1 (the yield from backscattered electrons approaching 1 and from true secondaries approaching zero) at zero primary energy as found in recent experimental data.<sup>6,25</sup> In contrast to measurements in Refs. 6 and 25 where a negative bias was applied to the sample to decelerate the primary electrons to low energy, measurements at PPPL will utilize an electron gun capable of producing primary electrons as low as 3eV. This will avoid the possibility of reflection of the primary electrons in the vacuum before reaching the sample. In addition, future experiments will investigate the sensitivity of the total yield to material temperature and will test the SEE of materials relevant to electric propulsion and fusion devices, including carbon-carbon composites.

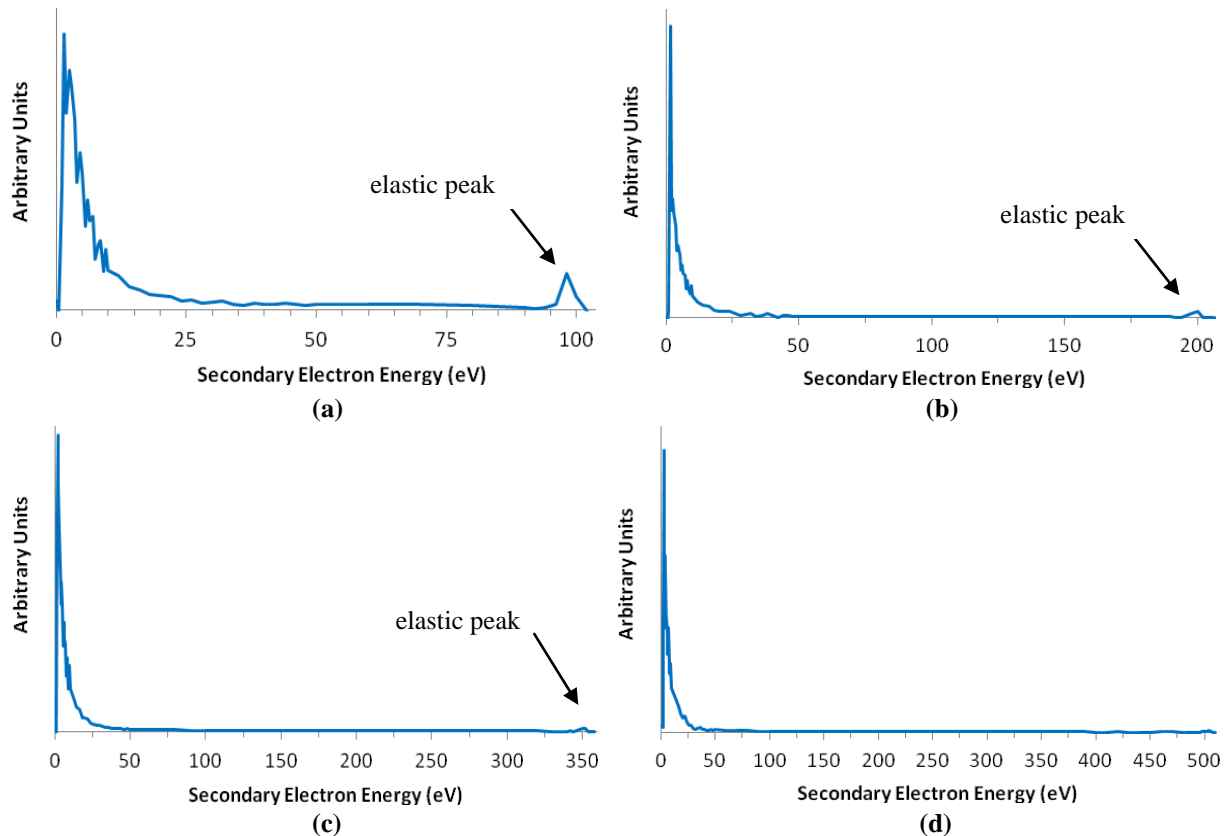


**Figure 8. Energy distributions of secondary electrons from a graphite sample due to electron bombardment at (a) 100eV, (b) 200eV, (c) 350eV, and (d) 500eV.**

### Acknowledgments

The authors would like to thank Dr. Angela Capece of the Material Science Program at the Princeton Plasma Physics Laboratory for much technical and scientific support, and Chenggang Jin for assistance in data collection. Funding for this research was provided by the Air Force Office of Scientific Research. This work was also supported in part by the University of Michigan/AFRL Center of Excellence in Electric Propulsion (MACEEP), Grant F9550-09-1-0695, with additional support from the UCLA School of Engineering and Applied Science.

### References

- <sup>1</sup> H. Seiler, "Secondary Electron Emission in the Scanning Electron Microscope," *Journal of Applied Physics*, Vol. 54, No. 11, 1983.
- <sup>2</sup> G. D. Hobbs and J. A. Wesson, "Heat Flow Through a Langmuir Sheath in the Presence of Electron Emission," *Plasma Physics*, Vol. 9, 1967, pp. 85-87.
- <sup>3</sup> J. P. Gunn, "Evidence for Strong Secondary Electron Emission in the Tokamak Scrape-off Layer," *Plasma Physics and Controlled Fusion*, Vol. 54, 085007, 2012.
- <sup>4</sup> D. Sydorenko, A. Smolyakov, I. Kaganovich, and Y. Raitses, "Kinetic Simulation of Secondary Electron Emission Effects in Hall Thrusters," *Physics of Plasmas*, Vol. 13, 014501, 2006.
- <sup>5</sup> D. Sydorenko, A. Smolyakov, I. Kaganovich, and Y. Raitses, "Effects of Non-Maxwellian Electron Velocity Distribution on Two-Stream Instability in Low-Pressure Discharges," *Physics of Plasmas*, Vol. 14, 013508, 2007.
- <sup>6</sup> R. Cimino, I. R. Collins, M. A. Furman, M. Pivi, F. Ruggiero, G. Rumolo, and F. Zimmermann, "Can Low-Energy Electrons Affect High-Energy Physics Accelerators?" *Physical Review Letters*, Vol. 93, No. 1, 2004.

- 
- <sup>7</sup> A. N. Andronov, A. S. Smirnov, I. D. Kaganovich, E. A. Startsev, Y. Raitses, and V. I. Demidov, "Secondary Electron Emission Yield in the Limit of Low Electron Energy," *Joint INFN-CERN-EuCARD-AccNet Workshop on Electron-Cloud Effects: E-CLOUD'12*, CERN-2013-002, 2013, pp. 161-163.
- <sup>8</sup> R. G. Lye and A. J. Dekker, "Theory of Secondary Emission," *Physical Review*, Vol. 107, No. 4, 1957, pp. 997-981.
- <sup>9</sup> J. R. M. Vaughan, "A New Formula for Secondary Emission Yield," *IEEE Transactions on Electron Devices*, Vol. 36, No. 9, 1989, pp. 1963-1967.
- <sup>10</sup> E. W. Thomas, "Particle-Impact Induced Electron Ejection from Surfaces," *International Nuclear Data Committee*, INDC(NDS)-322, 1995.
- <sup>11</sup> J. J. Scholtz, D. Dijkkamp, and R. W. A. Schmitz, "Secondary Electron Emission Properties," *Philips Journal of Research*, Vol. 50, 1996, pp. 375-389.
- <sup>12</sup> C. A. Ordóñez and R. E. Peterkin Jr., "Secondary Electron Emission at Anode, Cathode, and Floating Plasma-Facing Surfaces," *Journal of Applied Physics*, Vol. 79, No. 5, 1996, pp. 2270-2274.
- <sup>13</sup> J. M. Pedgley, G. M. McCracken, H. Farhang, and B. H. Blott, "Measurements of Secondary Electron Emission for Fusion Related Materials," *Journal of Nuclear Materials*, No. 196-198, 1992, pp. 1053-1058.
- <sup>14</sup> H. Fahang, E. Napchan, and B. H. Blott, "Electron Backscattering and Secondary Electron Emission from Carbon Targets: Comparison of Experimental Results with Monte Carlo Simulations," *Journal of Physics D: Applied Physics*, Vol. 26, 1993, pp. 2266-2271.
- <sup>15</sup> M. S. Chung and T. E. Everhart, "Simple Calculation of Energy Distribution of Low Energy Secondary Electrons Emitted from Metals Under Electron Bombardment," *Journal of Applied Physics*, Vol. 45, No. 2, 1974, pp. 707-709.
- <sup>16</sup> N. D. Zamerovski, P. Kumar, C. Watts, T. Svimonishvili, E. Schamiloglu, and J. A. Gaudet, "Secondary Electron Yield Measurements from Material with Application to Collectors of High-Power Microwave Devices," *IEEE Transactions on Plasma Science*, Vol. 34, No. 3, 2006, pp. 642-651.
- <sup>17</sup> M. Belhaj, J. Roupie, O. Jbara, J. Puech, N. Balcon, and D. Payan, "Electron Emission at Very Low Electron Impact Energy: Experimental and Monte-Carlo Results," *Joint INFN-CERN-EuCARD-AccNet Workshop on Electron-Cloud Effects: E-CLOUD'12*, CERN-2013-002, 2013, pp. 137-139.
- <sup>18</sup> M. E. Woods, B. J. Hopkins, and G. M. McCracken, "Secondary Electron Yield Measurements from Limiter Materials in the Joint European Torus," *Surface Science*, Vol. 162, 1985, pp. 928-933.
- <sup>19</sup> M. E. Woods, B. J. Hopkins, G. F. Matthews, G. M. McCracken, P. M. Sewell, and H. Farhang, "An Investigation of the Secondary-Electron Emission of Carbon Samples Exposed to a Hydrogen Plasma," *Journal of Physics D: Applied Physics*, Vol. 20, 1987, pp. 1136-1142.
- <sup>20</sup> R. E Kirby, "Instrumental Effects in Secondary Electron Yield and Energy Distribution Measurements," *31<sup>st</sup> ICFA Advanced Beam Dynamics Workshop on Electron-Cloud Effects: E-CLOUD'04*, CERN-2005-001, 2005, pp. 1-5.
- <sup>21</sup> D. M. Goebel, "High Voltage Breakdown Limits of Molybdenum and Carbon-based Grids for Ion Thrusters," *41<sup>st</sup> Joint Propulsion Conference*, AIAA-2005-4257, 2005.
- <sup>22</sup> S. P. Rawal, A. R. Perry, J. D. Williams, P. J. Wilbur, D. M. Laufer, W. Shih, J. Polaha, and W. A. Hoskins, "Performance Evaluation of 8-cm Diameter Ion Optics Assemblies Fabricated from Carbon-Carbon Composites," *40<sup>th</sup> Joint Propulsion Conference*, AIAA-2004-3614, 2004.
- <sup>23</sup> Y. Raitses, D. Staack, A. Dunaevsky, and N. J. Fisch, "Operation of a Segmented Electrode Hall Thruster with Low-Sputtering Carbon-velvet Electrodes," *Journal of Applied Physics*, Vol. 99, 036103, 2006.
- <sup>24</sup> S. Barral, S. Zurbach, and M. Dudeck, "Experimental Investigation of a Layered Graphite/BN Channel for Hall Thrusters," *32<sup>nd</sup> International Electric Propulsion Conference*, IEPC-2011-192, 2011.
- <sup>25</sup> R. Cimino and I. R. Collins, "Vacuum Chamber Surface Electronic Properties Influencing Electron Cloud Phenomena," *Applied Surface Science*, Vol. 235, 2004, pp. 231-235.